Materials Letters 126 (2014) 274–277

Contents lists available at ScienceDirect

Materials Letters

journal homepage: www.elsevier.com/locate/matlet

High T_c ferroelectricity in Ba-doped ZnO nanoparticles

Gunjan Srinet, Ravindra Kumar*, Vivek Sajal

Department of Physics and Materials Science and Engineering, Jaypee Institute of Information Technology, Noida 201307, Uttar Pradesh, India

ARTICLE INFO

Article history:
Received 6 February 2014
Accepted 9 April 2014
Available online 18 April 2014

Keywords:
Semiconductors
Ferroelectrics
Luminescence

ABSTRACT

Effects of Ba doping on structural, optical and ferroelectric properties of ZnO nanoparticles prepared by a low cost thermal decomposition method are presented. The substitution of Ba on Zn sites of the wurtzite structure of ZnO was observed by X-ray diffraction. Some structural transformation in the morphology of nanostructure with Ba doping was observed. Redshift in band gap is observed in the UV–visible spectra after Ba doping, supported by photoluminescence spectra and showing enhanced defect states with Ba doping. In dielectric studies, high value of dielectric constant and transition temperature at (~330 °C) were observed. High value of remnant polarization (1.01 $\mu C\,cm^{-2}$) and low value of coercive field (2.02 $kV\,cm^{-1}$) were also observed in ferroelectric studies which can be useful for potential applications.

1. Introduction

ZnO is a wide band gap (3.37 eV) semiconductor having unique features such as large exciton binding energy (60 meV) and large ferromagnetic and piezoelectric coefficients with a predicted curie temperature above room temperature when doped with the transition metal [1–3]. It is one of the potential semiconductors for developing blue and ultra violet (UV) photonic and spin photonic devices such as light emitting diodes (LED), laser diodes, solar blind UV photodetector, fast UV sensors and transparent electronic devices [4]. More interestingly, recent developments showed that doped ZnO is diluted magnetic semiconductor (DMS) which attracted considerable interest due to its potential application in spintronics [5]. There are several reports available in the literature on optical and magnetic properties of transition and non-transition metal doped ZnO [2,6], but still it is a good candidate for improving ferroelectric (FE) properties, which are of considerable importance in low dimensional ferroelectrics because of the demand for non-volatile FE memory device miniaturization [7,8]. Generally, pervoskites are used for FE memory devices which are structurally complicated and difficult to synthesize [9,10]. There are only few ZnO based FE materials reported in the literature which are highly controversial. Yadav et al. [11] observed dielectric anomaly at 430–460 K and claimed the anomaly not to be ferroelectric, Gupta et al. [12] reported ferroelectric transition around 343 K in K doped ZnO nanorods, Yang et al. [13] observed and explained the multiferrioc behavior of Cr doped ZnO. Recently, Gupta et al. [14] observed low ferroelectric phase transition at 69 °C.

Under this scenario, ferroelectric and dielectric properties of doped ZnO systems are highly interesting for scientific research. In this paper, we used a thermal decomposition method for the preparation of Ba doped ZnO nanoparticles and studied the structural, vibrational, optical, dielectric and ferroelectric properties. Further, till now, there are no reports available on ferroelectric studies of Ba doped ZnO nanoparticles.

2. Experimental details

Ba doped ZnO nanoparticles were synthesized by the thermal decomposition method by using chemicals of analytical grade. Initially, 0.16 mol $C_2H_5O_4 \cdot 2H_2O$ (oxalic acid) was dissolved in 100 ml of deionised (DI) water with vigorous stirring. Then, 0.02 mol diethanolamine (DEA) is added to get homogenous DEA/$C_2H_5O_4 \cdot 2H_2O$ solution (A). Now, 0.02 mol zinc nitrate was dissolved in 100 ml of DI water in which appropriate amount of barium nitrate (5%) was added to get the solution B. Finally, B was added dropwise in the aqueous solution A. White precipitates were formed and the suspension was continuously stirred at room temperature and kept for 12 h to settle down. Then, precipitates were filtered, washed with DI water and ethanol water several times, dried at room temperature and calcined at 500 °C for 2 h.

The crystalline structure and the phase purity of samples were confirmed by X-ray diffraction (XRD) measurements (Shimadzu XRD-6000 with CuKα ($\lambda = 1.5406$ Å) radiation). Absorption spectra were carried out by a Perkin ElmerLambda-35 UV–visible spectrometer in the wavelength range 300–800 nm. Photoluminescence (PL) spectra were acquired using xenon flash lamp laser as

---

* Corresponding author.
E-mail address: ravindrakbhatt@gmail.com (R. Kumar).

http://dx.doi.org/10.1016/j.matlet.2014.04.054
0167-577X/

excitation source by the Perkin Elmer Lambda luminescence spectrophotometer. Dielectric measurements were performed by impedance analyzer (Novocontrol) and PE loops were measured by P–E Loop Tracer (Marine India Ltd.).

3. Results and discussion

Rietveld refined XRD patterns of pure and Ba doped ZnO nanoparticles are shown in Fig. 1(i) in which all Bragg peaks are indexed in the wurtzite type hexagonal structure with space group P63mc [15]. It confirms that Ba doping has not altered the basic wurtzite crystal structure. Calculated refined parameters obtained after the final cycle of refinement are summarized in Table 1. Low values of χ^2 and profile parameters (R_p and R_{wp}) suggest the good quality of samples and effectiveness of refinement. Lattice parameters slightly increased after Ba doping, which can be assigned to a bigger ionic radius of Ba^{2+} than that of the Zn^{2+}, which shows the incorporation of Ba ions on Zn sites. Average crystallite sizes determined by Scherrer's formula were found to be 29 nm for pure ZnO and 25 nm for Ba doped ZnO sample, which is dependent on the increasing broadening of peaks with doping.

Microstructures investigated by FESEM show that the pure ZnO nanoparticle sample has a smooth surface with porous network (Fig. 1ii), due to the effect of surfactant (DEA) used during synthesis but grains are equally distributed in size and shape. Pure ZnO (Fig. 1 (ii a)) shows spherical shaped nanoparticles of small average grain size (80–100 nm), while, after Ba doping, small spherical grains are transformed to small cubes and rods with increased porosity (Fig. 1 (ii b and c)). It can happen as Ba ions get substituted in more number on the surface i.e. along '*c*' axis in the beginning. The surface Ba ions accelerate the growth by interparticle attraction during nucleation [16].

For the realization of ZnO based optical devices, band gap tuning is a prerequisite. In UV–visible spectra (Fig. 2a), a sharp absorption edge at around 375 nm, a characteristic of ZnO, is observed in both samples. It is observed that position of the absorption edge shifts towards higher wavelength side, indicating a decrease in the band gap with Ba doping. Band gap of samples was estimated by extrapolation of linear portion of $(\alpha h\nu)^2$ versus $h\nu$ curve (inset of Fig. 2a) by using the Tauc plot relation $\alpha \propto (h\nu - E_g)^{1/2}$ for direct band gap semiconductor between the absorption coefficient (α) and the energy band gap (E_g), where h is the Planks constant and ν is the frequency of incident photon. Band gaps are observed to be 3.18 eV for pure and 3.14 eV for Ba doped ZnO. This band gap contraction and the absorption edge redshift with 5% Ba doping may be attributed to the sp–d spin-exchange interactions between band electrons and the localized d electrons of the Ba ion substituting the cation. The s–d and p–d exchange interactions might have given negative and a positive correction to the conduction- and valence-band edges, respectively, resulting to the band-gap narrowing [17].

The room temperature PL spectra (Fig. 2b) for pure and Ba doped ZnO nanoparticles have shown two emission bands; one sharp emission in the UV region, corresponding to the near band edge (NBE) emission which is related to the recombination of free excitons between conduction and valence bands and other broad deep level emission in the visible region caused by impurities and structural defects which is only observed in Ba doped ZnO samples. Redshift in the NBE emission (around 390 nm) similar to shift in absorption edge in emission spectra was observed. Blue emission peaks at around 458 and 481 nm (inset of Fig. 2b) assigned to the energy of transition of electron from interstitial Zn (Zn_i) to Zn vacancies (V_{Zn}) [18] and to the transition between the oxygen vacancy and interstitial oxygen (O_i), respectively and the emission peak observed at 422 nm can be attributed to the energy of transition of electron from the bottom of conduction band to O_i level [19]. The green emission peak (~505 nm) could be due to the transition from Zn_i levels to O_i. The debatable emission around 524 nm may be due to several type of defects such as V_o (oxygen vacancies), Zn_i, V_{Zn} and O_i [20]. Thus, it can be concluded that the Ba-doping leads to redshift in NBE and increase in intrinsic defects such as V_o and O_{Zn} density.

FTIR transmittance spectra (Fig. 2c) encompass several important stretch modes involving hydrogen bonding to carbon as well as to oxygen and ZnO bonding. An absorption band revealing

Table 1
Calculated parameters from refinement.

Samples	Lattice parameters			Bond length (Å)	*R*-factors					
	a=*b* (Å)	*c* (Å)	*V* (Å)^3		R_p	R_{wp}	R_{exp}	χ^2	R_b	R_f
Pure ZnO	3.248	5.208	47.604	1.977	11.1	10.8	6.8	2.5	2.21	2.2
5%-Ba	3.249	5.211	47.642	1.979	10.0	9.95	5.92	2.8	1.94	1.2

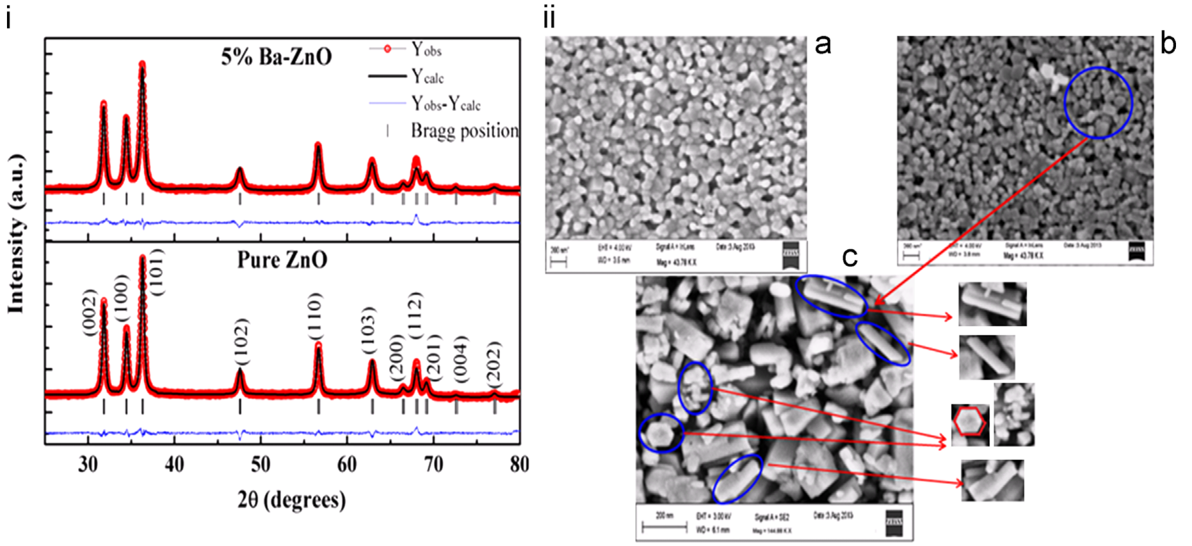

Fig. 1. (i) Reitveld refined XRD patterns of pure and Ba doped ZnO nanoparticles. (ii) FESEM image of (a) pure and (band c) 5% Ba doped ZnO with different resolutions.